Joint International Topical Meeting on Mathematics & Computation and Supercomputing in Nuclear Applications (M&C + SNA 2007)
Monterey, California, April 15-19, 2007, on CD-ROM, American Nuclear Society, LaGrange Park, IL (2007)

VHTR NUMERICAL BENCHMARK BASED ON THE COMPACT NUCLEAR POWER SOURCE EXPERIMENTS

Hyung-Kook Joo,* Temitope A. Taiwo and Won Sik Yang
Argonne National Laboratory
9700 South Cass Avenue, Argonne, Illinois, USA
hkjoo@anl.gov; Taiwo@anl.gov; wyang@anl.gov

ABSTRACT

Two- and three-dimensional numerical benchmark cases based on the Compact Nuclear Power Source (CNPS) experiments conducted at the Los Alamos National Laboratory (LANL) in the 1980s have been specified for the validation and verification of Very High Temperature Reactor (VHTR) physics codes. Previous evaluation of the CNPS experiments has shown that the experimental tests could be useful for the validation of neutronic data and codes developed for the analysis of VHTR cores and that the Monte Carlo results obtained for critical test configurations are representative of the neutronic characteristics of the CNPS. To define the benchmark cases that could be readily analyzed by current deterministic lattice and whole-core physics codes, the irregular arrangement of channels in the actual CNPS core was simplified to a regular Cartesian geometry arrangement in the benchmark cases, while preserving the important neutronic characteristics of the CNPS. The results of deterministic calculations using HELIOS/DIF3D were compared to MCNP4C Monte Carlo results to show the usefulness of the numerical benchmark cases.

Key Words: Numerical Benchmark, VHTR, CNPS, Critical Experiment, Reactor Physics

1. INTRODUCTION

Previous evaluation [1] of the CNPS experiments [2,3,4,5] has shown that the experimental tests could be useful for the validation of neutronic data and codes developed for the analysis of VHTR cores. The study also revealed that MCNP4C [6] Monte Carlo calculations give results that are representative of the neutronic characteristics of the CNPS. The lack of information on design data uncertainties and the inconsistency in the design data from different sources make it difficult to quantify the uncertainty in the core integral parameters arising from design data uncertainties. The evaluated configurations could however be useful as numerical benchmarks that are based on the currently available information. It was therefore decided to specify benchmark problems based on these tests from the information available in the open literature. [2,3,4,5]

The irregular arrangement of the fuel channels however made it impractical to define useful heterogeneous problems for current deterministic codes that would contain detailed representation of the channels in their actual locations. Consequently, it was decided to change the irregular channel arrangement in order to define whole-core problems for deterministic codes that would preserve the important physics characteristics of the CNPS cores. A regular Cartesian

*Permanent address: Korea Atomic Energy Research Institute, 150 Deokjin-dong, Yuseong, Deajeon, Korea; hkjoo@kaeri.re.kr

geometry arrangement of the channels and core internals was found to be the best option. Additional simplifications to the CNPS geometry and composition of the graphite blocks were also made to remove complications in the benchmark specification. Using this approach, 2-D and 3-D benchmark cases have been defined for two critical configurations of the CNPS that have 184 and 492 fueled channels. For the 2-D benchmark configuration, an axially infinite core was assumed. In addition to the axially infinite core representation, partially inserted B_4C shim and control rod are axially homogenized by diluting B_4C number densities for the 2-D representation of the core with 492 fueled channels.

In this paper, a brief description of the CNPS core is provided. The transformation of the original core into benchmark cases useful for validating deterministic tools is then discussed. This was done using MNCP models to sequentially reduce the fuel channel arrangement from the irregular cylindrical geometry to the Cartesian geometry arrangement, preserving most of the neutronic characteristics of the CNPS. The simplifications to geometry and composition were also made to remove complications in benchmark specification. Finally, to test the specified numerical benchmark cases, a deterministic code package of HELIOS[7]/DIF3D[8] is applied to solve the benchmark cases and the solutions of HELIOS/DIF3D are compared to MCNP4C results.

2. DESCRIPTION OF CNPS CORES AND EXPERIMENTS

The CNPS was a small reactor system designed to provide power at sites where fuel costs and logistics make fossil-fuel-powered systems less attractive. The CNPS design used TRISO fuel particles and could produce 20 KWe continuously for 20 years without refueling and be walk-away safe; the core had an inherently large negative temperature reactivity coefficient and relied on the stability of the TRISO fuel particle at the highest temperature anticipated following a maximum credible accident. Due to the size and weight constraints, the CNPS was criticality limited and its ability to remain critical for the life of the core had to be verified. Thus, physics experiments were conducted at the Los Alamos National Laboratory (LANL) for this purpose. The CNPS was designed to use a heterogeneous uranium graphite cylindrical core, depicted schematically in Figure 1. The core height was 113 cm and the diameter was 120 cm. The CNPS core was reflected both radially and axially with graphite. The core and bottom reflector were supported by a 6 cm thick aluminum plate. The core contained 492 fuel channels, 5 control rod channels, and 12 heat pipe channels as shown in Figure 1. Twenty extra channels were also available near the core center for the placement of beryllium to increase core reactivity, but they were filled with graphite for all the experiments conducted. Each fuel channel or extra channel had a diameter of 1.285 cm.

Different critical configurations were obtained by loading different number of fuel channels with uncladded fuel compacts containing the TRISO fuel particles in a graphite matrix with a $C/^{235}U$ atomic ratio of 3000 (i.e., C/U ~ 600); low-enriched uranium (19.9% U-235) oxy-carbide fuel was used. The control rod channels had a diameter of 3.494 cm and penetrated the upper reflector axially. The heat pipe channels had a diameter of 6.185 cm and similarly penetrated the upper reflector. The requirement of ensuring a minimum web thickness between any two free surfaces made it difficult to maintain a constant fuel element pitch. To minimize this problem, the fuel channels were arranged in an irregular lattice with a 45-degree azimuthal symmetry. The active core height was 108.46 cm, which is less than the height of the core block (113 cm).

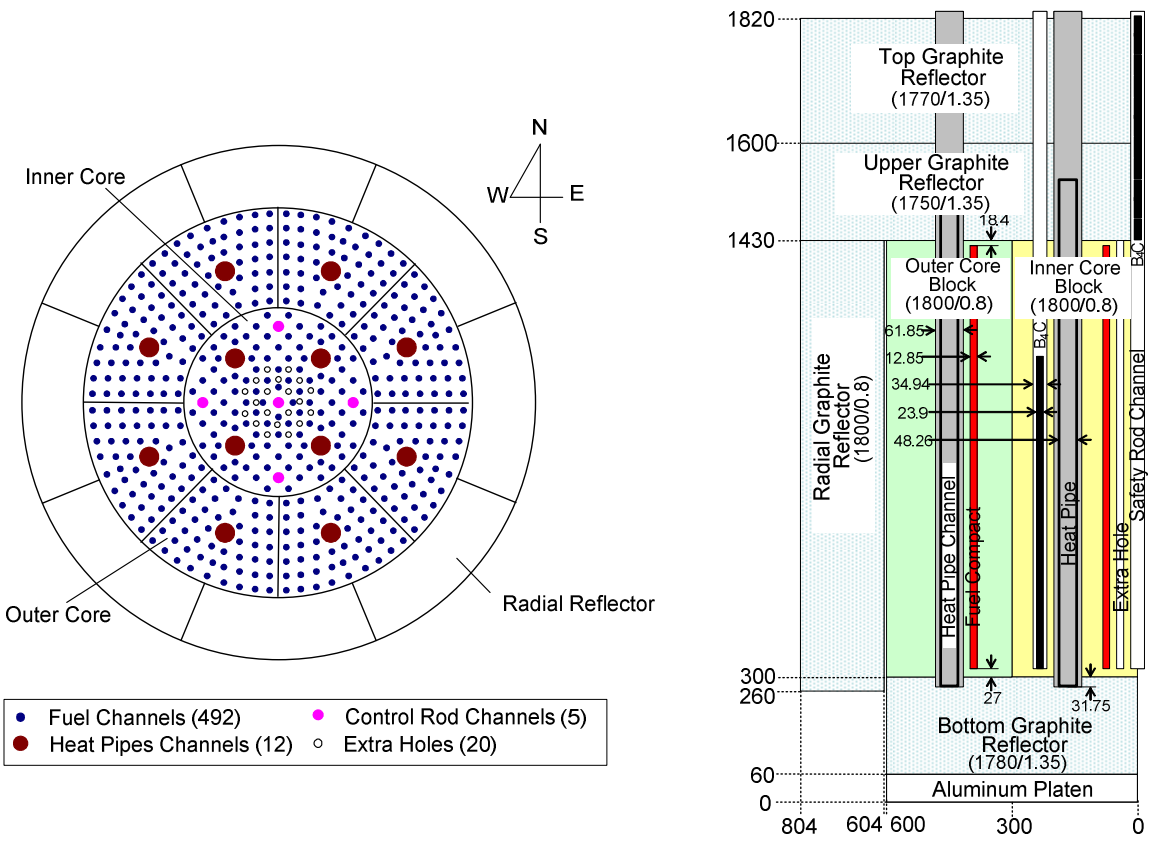

Figure 1. Planar and Vertical Views of CNPS Core (Dimensions in mm).

Critical state measurements were conducted under the CNPS experimental program. Four critical loadings contained 184, 202, 380, and 492 fueled channels with different loading of pellets, simulated heat pipes, and shim rod.[2] In addition, experiments were performed to determine material worths, safety rod worth, shim differential worths, temperature reactivity coefficients, and power profiles (using foil activation techniques).

3. NUMERICAL BENCHMARK BASED ON CNPS EXPERIMENTS

3.1 Development of Numerical Benchmark

An irregular cylindrical arrangement of channels was used for the CNPS core due to the presence of control rod, heat pipe and extra hole channels (Figure 1). To facilitate the use of the CNPS experimental data for the validation of current deterministic tools for VHTR core analysis, it was decided to simplify the problem geometry, while preserving the core physics characteristics. To make the benchmark cases solvable by a large group of potential participants, a regular arrangement of channels in Cartesian geometry was defined as shown in Figure 2. This was done by adjusting the relative positions of the fuel rod channels, control rod channels, and heat pipe channels. The numerical benchmark cases preserve the number of each type of channels in a given experimental configuration. The basic benchmark configuration consists of 492 fuel channels, five control rod channels, and twelve heat pipe channels. Each cell containing a channel has a square pitch of 4.7138 cm. The radial reflector surrounding the core was also defined in Cartesian geometry, preserving approximately the area of the radial reflector. The

positions of heat pipe and control rod channels for the numerical benchmark cases were determined such that the core multiplication factor and reactivity worths (control rod, shim rod, and heat pipe worths) of the original CNPS configurations were preserved. The derived positions are shown in Figure 2.

Four compositions with different densities and impurities were used for the graphite block in CNPS experiment: core and radial reflector block, bottom reflector, upper reflector, and top reflector. The densities and impurities of graphite blocks were different only slightly from each other, thus the composition of the core graphite block was used for simplicity for the other graphite blocks in the benchmark specification. The effect of this simplification was evaluated and found to be not so large; increased k_{eff} about 220 pcm for the 184 fueled-channel core and 150 pcm for the 492 fueled-channel core.

The original outer diameter of the heat pipe (6.185 cm) is larger than the side length of the cell defined in the numerical benchmark cases. Therefore, the heat pipe diameter was reduced to fit into a square cell, while preserving the mass. The effect of the reduced heat pipe diameter was calculated with MCNP4C for the original core configuration. The reduced heat pipe diameter increased k_{eff} by ~1700 pcm for the 184 fueled-channel core and ~1200 pcm for the 492 fueled-channel core. Additional simplifications to the CNPS geometry were also made to remove complications for groups analyzing the benchmark. These additional simplifications include: (1) leveling the bottom positions of the heat pipe, control rod, and fuel compact channels, (2) excluding the radial gap between the core and the radial reflector, (3) extending the bottom aluminum plate and radial reflector, and (4) replacing with graphite the heat pipe and control rod channel zones extending into the reflector. The resulting axial configurations are simplified as shown in Figure 3. The reactivity effects of the simplified geometry were calculated both with the original configuration and the numerical benchmark configuration. The combined effect of the geometry simplifications including reduced heat pipe size was found to be an increase of about 3.5 to 4% in the k_{eff} values of the 184 and 492 fueled-channel cores.

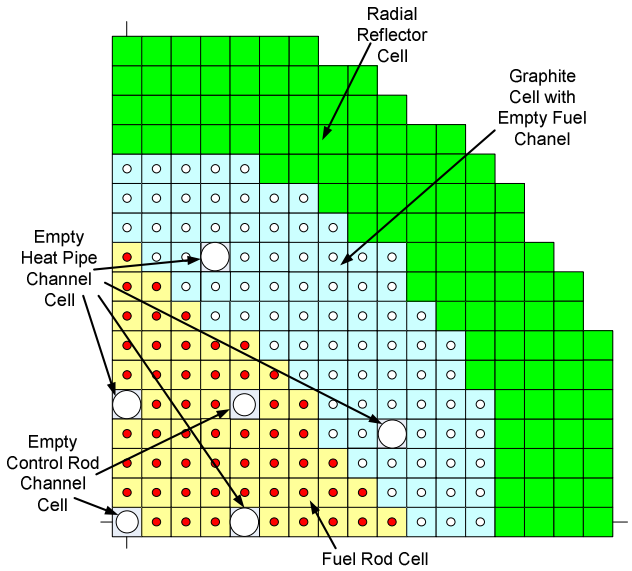

Figure 2. Benchmark Configuration of 184 Fueled-Channel Core.

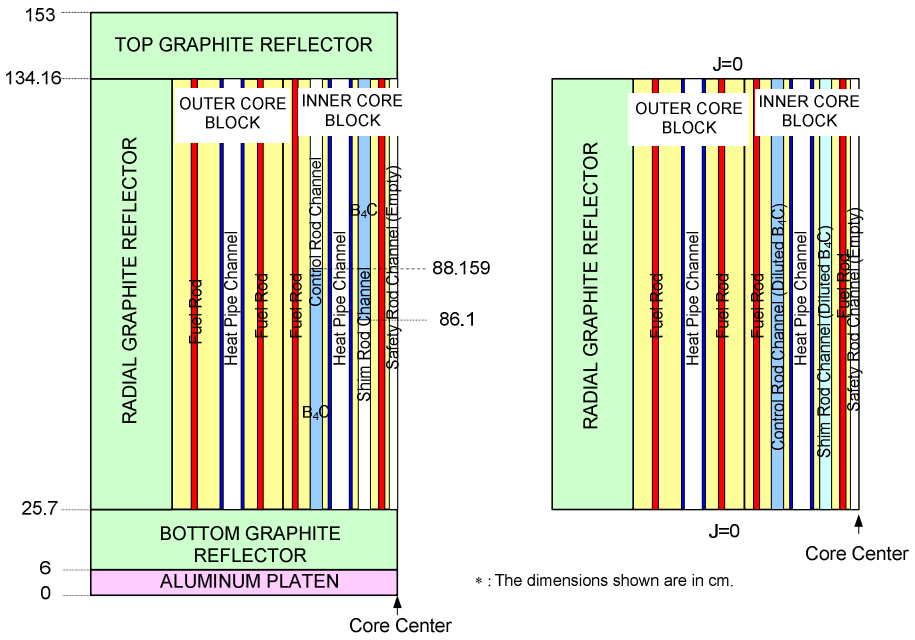

Figure 3. Axial Configurations of 3-D and 2-D Benchmarks for 492 Fueled-channel Core.

Because the numerical benchmark includes the effect of geometry simplification, the k_{eff} of the benchmark system is far from critical. It is preferable to keep the k_{eff} of the numerical benchmark close to critical state to retain the spectral characteristics of the critical experiments. The thicknesses of the bottom and top reflectors were reduced to make the k_{eff} of the benchmark cases close to unity by enhancing the leakage through the top and bottom reflectors. It was confirmed that this modification resulted in the lowest (and insignificant) perturbation to the neutron spectrum, of all the various approaches investigated for reducing the k_{eff} of the simplified geometry.

The specification of the 2-D benchmark required additional approximations. For example, the axially heterogeneous configuration resulting from the partial insertion of shim rod and control rods in the 492 fueled-channel core cannot be directly modeled with a 2-D code. Thus, the axial homogenization of control rods and shim rod by diluting the B_4C material was done in order to specify the 2-D problems. The diluted B_4C number densities were determined such that the k_{eff} and the radial power distribution of the partially rodded cores were preserved.

3.2 Specification of Numerical Benchmark

The numerical benchmarks based on the CNPS experiments have been specified for two cases: 184 fueled-channel core (CNPS-184) and 492 fueled-channel core (CNPS-492). The CNPS-184 configuration is composed of 184 fuel cells, one empty safety rod channel cell at the center of core, four empty control rod channel (including one empty shim rod channel) cells, twelve empty heat pipe channel cells, 308 graphite cells with empty fuel channel, and 404 graphite reflector cells as shown in Figure 2. The radial core configuration for the CNPS-492 case is presented in Figure 4. The CNPS-492 configuration is composed of 492 fuel cells, one empty safety rod channel, three control rod channels and one shim rod channel in symmetric positions, twelve heat pipe channels, and 404 graphite reflector cells. Each cell in both the CNPS-184 and CNPS-492

cores has a square shape. The axial configuration for the CNPS-492 core is given in Figure 3. For the 3-D benchmark problem, a top graphite reflector, a bottom aluminum platen and a bottom graphite reflector are included in the configuration. The control rod and shim rod are also partially inserted as shown in Figure 3. In the CNPS-492 core configuration, three control rods are partially inserted from the bottom of the core to 62.459 cm above the core bottom and one shim rod is partially inserted by 48.06 cm from the top of the core. The control rod and shim rod in 2-D benchmark for CNPS-492 core are axially homogenized by diluting the number density of B_4C. The 2-D benchmark problem is composed of an axially infinite core region. Since all the control rod channels are empty in the configuration for the 184 fueled-channel core, the control rod insertion region in Figure 3 is replaced by void for the axial configuration for the CNPS-184 core.

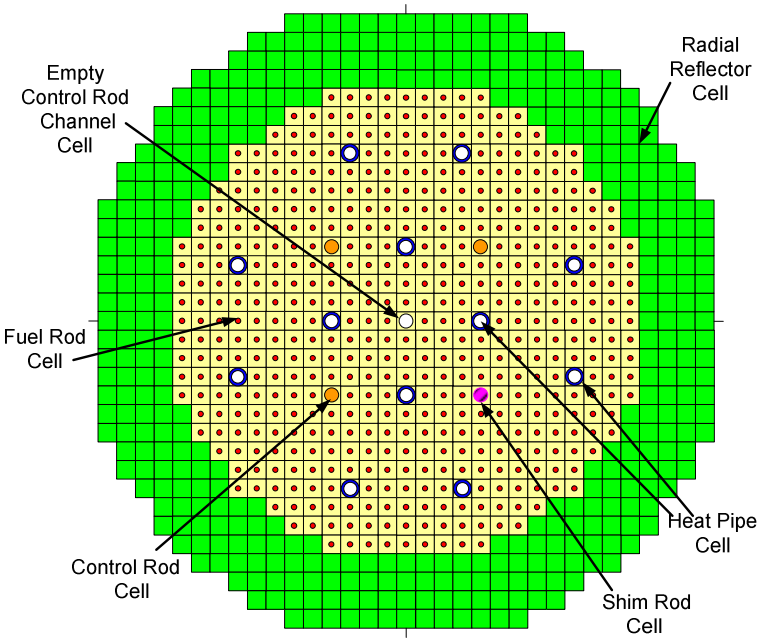

Figure 4. Benchmark Configuration of CNPS-492 Core.

The side length of each square cell is 4.7138 cm. The fuel cell is composed of the fuel compact, graphite moderator, and the gap between fuel compact and graphite moderator. The graphite cell with empty fuel channel, control rod channel cell and heat pipe channel cell for CNPS-184 are composed of empty channel and graphite block. The cell for the control rod inserted region in CNPS-492 is composed of control rod, control rod tube, gaps between control rod and graphite block, and graphite block. For the shim-rod inserted region, the cell is composed of the shim rod, shim rod tube, the gap between shim rod tube and graphite block, and graphite block. The radial reflector, axial reflector, and aluminum platen cells have a solid square cell without channel.

The dimension of each cell and the number density of the region bearing different materials are listed in Table I. For the fuel cell, the homogeneous fuel compact model only is given in this paper. Even though the particle fuel model was also specified in the benchmark [9], the particle

heterogeneity effect for this benchmark was small due to the high moderator-to-fuel ratio and high fuel packing fraction. Reference 2 also reported that the reactivity effect of grain shielding (heterogeneity effect) was calculated by General Atomics Technology to be on the order of 200 to 300 pcm. The diluted B_4C number densities of the control rod and the shim rod for the 2-D benchmark problem are also provided in Table II.

The parameters to be calculated and compared for the benchmark cases are the k_{eff} value, axial and radial power distributions, and shim and control rod worths. The reference solutions for the numerical benchmarks were calculated with MCNP4C using ENDF/B-VI library and provided in Reference 9. Some of these solutions (k_{eff} values for 2-D and 3-D cores, radial power distribution for CNPS-184 and material worths) are also presented in Section 3.3.

Table I. Specification of Cells in CNPS Benchmark Cases

Cell	Region	Outer Radius (cm)	Isotope	Number Density (#/barn-cm)
Fuel	Fuel Compact	0.6225	U-235 U-238 O C Si B-10 B-11	5.67432 E-04 2.25514 E-03 4.79836 E-03 4.83268 E-02 5.40920 E-03 5.51315 E-08 2.24015 E-07
	Gap	0.6425	O	1.00000 E-09
	Graphite Block	-	C B-10 B-11	9.02516 E-02 1.58399 E-08 6.43622 E-08
Empty Fuel Channel	Void	0.6425	O	1.00000 E-09
	Graphite Block	-	Same as Fuel Cell	
Empty Control Rod Channel	Void	1.747	O	1.00000 E-09
	Graphite Block	-	Same as Fuel Cell	
Empty Heat Pipe Channel	Void	2.300	O	1.00000 E-09
	Graphite Block	-	Same as Fuel Cell	
Graphite Reflector	Graphite Block	-	Same as Fuel Cell	
Aluminum Platen	Aluminum	-	Al	6.02626 E-02
Stainless Steel Heat Pipe	Void	1.91035	O	1.00000 E-09
	SS-316 Heat Pipe	2.300	C Mn Si Cr Ni Mo P S Fe	3.14582 E-04 1.71937 E-03 1.68163 E-03 1.54416 E-02 9.65618 E-03 1.23070 E-03 6.86170 E-05 4.41879 E-05 5.52639 E-02
	Graphite Block	-	Same as Fuel Cell	

Table II. Specification of Control and Shim Rod Cells in CNPS Benchmark Cases

Cell	Region	Outer Radius (cm)	Isotope	Number Density (#/barn-cm)
Control Rod	B_4C (for 3-D Core)	1.195	C B-10 B-11	2.51856 E-02 1.98966 E-02 8.08456 E-02
	Gap	1.4	O	1.00000 E-09
	Control Rod Tube	1.5	Al	6.02626 E-02
	Gap	1.747	O	1.00000 E-09
	Graphite Block	-	C B-10 B-11	9.02516 E-02 1.58399 E-08 6.43622 E-08
	B_4C (for 2-D Core)	1.195	C B-10 B-11	8.23156 E-04 6.50293 E-04 2.64233 E-03
	Enriched B_4C (for Safety Rod Worth Calculation only)	1.195	C B-10 B-11	2.52175 E-02 5.53575 E-02 4.55125 E-02
Shim Rod	B_4C (for 3-D Core)	0.6285	C B-10 B-11	9.69892 E-03 7.66215 E-03 3.11335 E-02
	Shim Rod Tube	0.8825	Al	6.02626 E-02
	Gap	1.747	O	1.00000 E-09
	Graphite Block	-	Same as Control Rod Cell	
	B_4C (for 2-D Core)	0.6285	C B-10 B-11	7.26031 E-04 5.73564 E-04 2.33056 E-03

3.3 Results of Test Calculations

In order to test the specified numerical benchmark cases, deterministic calculations using lattice and whole-core analysis codes have been performed for the CNPS numerical benchmark cases. The whole-core calculations using HELIOS [7] with 47-group library were performed to generate the macroscopic cross sections for each lattice cell. The macroscopic cross sections for each cell were determined by flux-and-volume weighting over all the cells of each type of cells in the core. Whole-core DIF3D results have been obtained using the 47-group cross-sections generated from HELIOS calculations. The DIF3D calculations using both the DIF3D-VARIANT (nodal transport) [10] and DIF3D-nodal (nodal diffusion) [8] options have been performed. The k_{eff} values calculated with DIF3D for the 2-D and 3-D benchmark cases, with the VARIANT P-1, P-3, and P-5 options for angular approximation of flux and DIF3D-nodal are summarized in Table III. The anisotropic scattering was approximated with transport corrected P_0 scattering cross sections for all calculations. The reference MCNP4C results are also provided for comparison.

Table III. k_{eff} Values of Deterministic Calculations for CNPS Benchmark

			184 Fueled-Channel Core	492 Fueled-Channel Core
2-D Core	MCNP4C (with Homogeneous Fuel Compact Model)		1.19555	1.15799
	HELIOS/DIF3D (47-g)	Nodal Diffusion	1.19717	1.14622
		VARIANT P-1	1.19547	1.14470
		VARIANT P-3	1.19928	1.15348
		VARIANT P-5	1.19965	1.15485
3-D Core	MCNP4C (with Homogeneous Fuel Compact Model)		1.00164	1.00378
	HELIOS/DIF3D (47-g)	Nodal Diffusion	1.00387	0.99319
		VARIANT P-1	1.00235	0.99181
		VARIANT P-3	1.00897	1.00167
		VARIANT P-5	1.00977	NA

The highest order HELIOS/DIF3D calculation (P-5) gives k_{eff} values that are within 0.34% of the MCNP4C results for both the 184 and 492 fueled-channel 2-D cores; an overestimation of ~0.34 %Δk for the 184 fueled-channel core and an underestimation of ~0.27 %Δk for the 492 fueled-channel core. The discrepancy of the k_{eff} between the 47-group DIF3D diffusion calculation and the MCNP4C calculation is ~0.14 %Δk for the 184 fueled-channel core and ~0.98 %Δk for the 492 fueled-channel core. The larger discrepancies of diffusion solutions are mainly due to the transport effect. The transport effect estimated by subtracting the k_{eff} of the P-1 solution from that of the P-5 solution is ~0.35 %Δk for the 184 fueled-channel core and ~0.85 %Δk for the 492 fueled-channel core. For the 3-D benchmark case, the results of HELIOS/DIF3D calculation show a similar trend as in the 2-D core case; an overestimation for 184 fueled-channel core and an underestimation for 492 fueled-channel core. The discrepancy of the k_{eff} between the 47-group DIF3D diffusion calculation and MCNP4C calculation is similar to that for the 2-D benchmark cases; ~0.22 %Δk for the 184 fueled-channel core and ~1.06 %Δk for the 492 fueled-channel core. A larger transport effect (~0.74 %Δk) than in the 2-D case is observed for 184 fueled-channel core.

The radial power distributions for the 2-D and 3-D cores of CNPS-184 and CNPS-492 have also been calculated with HELIOS/DIF3D. The power distributions for CNPS-184 only are presented in this paper as Figures 5 and 6. The power distributions calculated by HELIOS/DIF3D with the P-5 option agree well with those from MCNP4C calculations; the RMS error is ~0.25% for the CNPS-184 case and ~0.80% for the CNPS-492 case for both the 2-D and 3-D cores. The power distribution calculated by the diffusion option also shows good agreement with MCNP4C results. The difference between the power distributions with the P-5 (or P-3) option and the diffusion option is less than 1% except the cells around control or shim rods where the power distribution calculated with the diffusion option shows a remarkable dips, but less than 2%. Although the axial power distributions for the 492 fueled-channel core is not presented in this paper, it is noted the axial power calculated by HELIOS/DIF3D agrees well with that of the MCNP4C calculation. The axial power from the HELIOS/DIF3D calculation captures well the slightly top-skewed shape which is caused by the partial insertion of control rods.

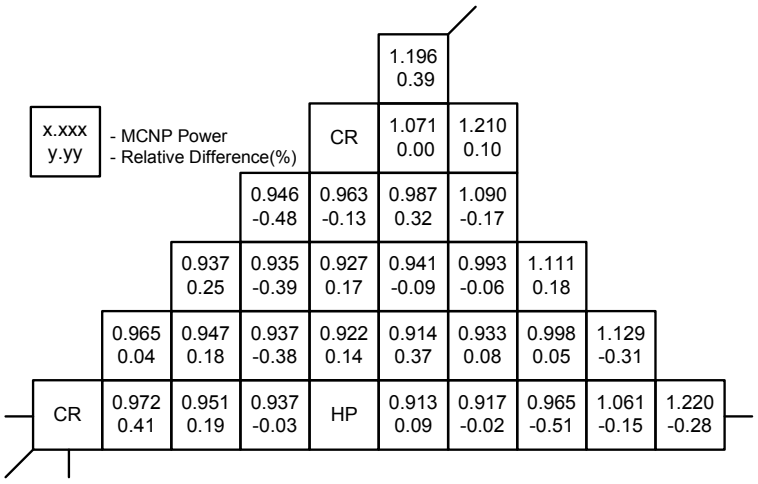

Relative Difference = (HELIOS/DIF3D-MCNP)/MCNP*100%
DIF3D with VARIANT P-5 Option
Maximum relative difference = 0.51%, RMS difference = 0.25%

Figure 5. Power Distribution Comparison for CNPS-184 2-D Benchmark Case.

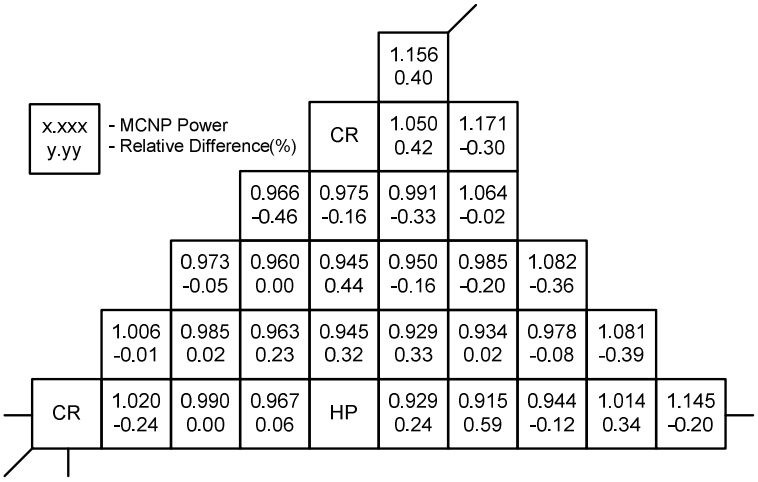

Relative Difference = (HELIOS/DIF3D-MCNP)/MCNP*100%
DIF3D with VARIANT P-5 Option
Maximum relative difference = 0.59%, RMS difference = 0.28%

Figure 6. Power Distribution Comparison for CNPS-184 3-D Benchmark Case.

The material worths have been calculated with HELIOS/DIF3D for the 3-D core model and the results are summarized in Table IV. The nodal diffusion option only was used due to computer memory limitation. The HELIOS/DIF3D-nodal calculation overestimates the safety rod worth and shim rod worth by about 10%. An additional calculation with the P-5 option for safety rod worth of the CNPS-184 gives 10.09, which agrees very well with the MCNP4C result within ~3.4%. This result indicates that the overestimation of the control and shim rod worths by ~10% mainly due to the diffusion theory approximation used in the calculation. For the CNPS-184 core, the stainless steel heat pipe worths calculated with DIF3D also agreed well with the MCNP4C values within 3%.

Table IV. Comparison of Safety Rod, Shim Rod, and SS Heat Pipe Worths

Parameters		MCNP4C	HELIOS/DIF3D (Diffusion Nodal)
Safety (Central) Control Rod Worth ($)	CNPS-184 Core - Natural B_4C	9.75 ± 0.097	10.84*
	CNPS-492 Core - Natural B_4C	5.51 ± 0.090	6.01
	- Enriched B_4C	6.11 ± 0.093	6.77
B_4C Shim Rod Worth ($)	CNPS-184 Core	2.78 ± 0.093	3.12
	CNPS-492 Core	2.32 ± 0.089	2.52
SS Heat Pipe Worth (¢/kg)	CNPS-184 Core - Heat Pipe in inner core	-34.08 ± 0.411	-35.04**
	- Heat Pipe in outer core	-19.75 ± 0.204	-20.29**

* Safety rod worths for CNPS-184 are 10.18 with P-3 and 10.09 with P-5 options.
** Heat pipe (HP) worths for CNPS-184 with P-5 option are 34.76 for inner and 19.60 for outer HPs.

4. CONCLUSIONS

Numerical benchmark cases based on the CNPS experiments have been specified for the verification and validation of VHTR deterministic physics codes. The original configurations of the CNPS core that used irregular arrangements of channels were transformed into those with regular Cartesian geometry arrangements of channels for the purpose of simplifying the geometry for deterministic code calculations. Preserving the CNPS core physics characteristics was a requirement for this transformation. Additional simplifications to the CNPS geometry and the composition of graphite blocks were also made to remove complications in benchmark specification. Using this approach, 2-D and 3-D benchmark cases were defined for two critical configurations, CNPS-184 and CNPS-492. The parameters calculated and compared for the benchmark cases were the k_{eff}, axial and radial power distributions, and shim and control rod worths.

The specified numerical benchmark cases were analyzed using deterministic two-step calculations with lattice and whole-core analysis codes, HELIOS and DIF3D, respectively. The k_{eff} values and the radial power distributions calculated using HELIOS/DIF3D with 47-group cross sections were found to be in good agreement with those obtained with MCNP4C as reference solutions. The k_{eff} values of HELIOS/DIF3D transport calculations with P-5 option agreed with the MCNP4C results within 0.34 $\%\Delta k$ for the 2-D core and 0.81 $\%\Delta k$ for the 3-D core of the CNPS-184 and CNPS-492 configurations. The power distributions calculated by

HELIOS/DIF3D with the P-5 option agreed well with those from MCNP4C calculations; the RMS error is ~0.25% for the CNPS-184 case and ~0.80% for the CNPS-492 case for both 2-D and 3-D cores. It was also found that considerable transport effects exist in these benchmark cases, particularly for the CNPS-492 2-D core and the 3-D cores of the CNPS-184-and CNPS-492 cases. Additionally, the material worths from HELIOS/DIF3D transport calculations agreed very well with the MCNP4C results within ~3.4%. The results of benchmark test calculations with deterministic codes show that the numerical benchmark cases presented in this paper are reasonably specified.

ACKNOWLEDGEMENTS

This work was supported by the U.S. Department of Energy under Contract number DE-AC02-06CH11357. The Korea Atomic Energy Research Institute (ROK) support for this work is also greatly appreciated.

REFERENCES

1. T. A. Taiwo, W. S. Yang, T. K. Kim, and H. S. Khalil, and H. K. Joo and S. J. Kim, "Preliminary Evaluation of the Compact Nuclear Power Source (CNPS) Critical Experiments as a VHTR Physics Benchmark," *Proc. PHYSOR 2006 – Advances in Nuclear Analysis and Simulation*, Vancouver, British Columbia, Canada, September 10-14, on CD-ROM (2006).
2. G. E. Hansen and R. G. Palmer, "Compact Nuclear Power Source Critical Experiments and Analysis," *Nucl. Sci. Eng*., **103**, pp.237-246 (1989).
3. R. G. Palmer, "Postanalysis of the CNPS Critical Experiments," *Proc. Int'l. Reactor Physics Conference*, Jackson Hole, Wyoming, September 18-21 (1988).
4. G. E. Hansen, J. H. Audas, E. R. Martin, R. A. Pederson, G. D. Spriggs, and R. H. White, "Critical Experiments in Support of the CNPS Programs," *Proc. Int'l. Reactor Physics Conference*, Jackson Hole, Wyoming, September 18-21 (1988).
5. R. G. Palmer and J. W. Durkee Jr., "Neutronic Design Studies for and Unattended, Low Power Reactor," *Proceeding of ANS Topical Meeting on Reactor Physics and Safety*, Saratoga Springs, New York, September 17-19 (1986).
6. J. F. Briesmeister, "*MCNP – A General Monte Carlo N-Particle Transport Code, Version 4C*," LA-13709-M, Los Alamos National Laboratory, April (2000).
7. R. J. Stamml'er et al., "*HELIOS Methods*," Studsvik Scandpower (1998).
8. R. D. Lawrence, "*The DIF3D Nodal Neutronics Option for Two- and Three-Dimensional Diffusion Theory Calculations in Hexagonal Geometry*," ANL-83-1, Argonne National Laboratory, Argonne, Illinois (1983).
9. H. K. Joo, T. A. Taiwo, and W. S. Yang, "*Numerical Benchmark Based on the Compact Nuclear Power Source (CNPS) Critical Experiments*," ANL-GenIV-090, Argonne National Laboratory, Argonne, Illinois (2006).
10. G. Palmiotti, "*VARIANT: Variational anisotropic nodal transport for multidimensional cartesian and hexagonal geometry calculation*," ANL-95/40, Argonne National Laboratory, Argonne, Illinois (1995).